

# High-temperature nonequilibrium Bose condensation induced by a hot needle

Alexander Schnell,<sup>1,\*</sup> Daniel Vorberg,<sup>1</sup> Roland Ketzmerick,<sup>1,2</sup> and André Eckardt<sup>1,†</sup>

<sup>1</sup>Max-Planck-Institut für Physik komplexer Systeme, Nöthnitzer Straße 38, 01187 Dresden, Germany

<sup>2</sup>Technische Universität Dresden, Institut für Theoretische Physik and Center for Dynamics, 01062 Dresden, Germany  
(Dated: May 17, 2022)

We investigate theoretically a one-dimensional ideal Bose gas that is driven into a steady state far from equilibrium via the coupling to two heat baths: a global bath of temperature  $T$  and a “hot needle”, a bath of temperature  $T_h \gg T$  with localized coupling to the system. Remarkably, this system features finite-size Bose condensation at temperatures  $T$  that are orders of magnitude larger than the equilibrium condensation temperature. This counterintuitive effect is explained by a suppression of long-wavelength excitations resulting from the competition between both baths. Moreover, for sufficiently large needle temperatures ground-state condensation is superseded by condensation into an excited state, which is favored by its weaker coupling to the hot needle. Our results suggest a general strategy for the preparation of quantum degenerate nonequilibrium steady states with unconventional properties and at large temperatures.

**Introduction.**—In thermal equilibrium the state of a system is strongly restricted by the laws of thermodynamics. Irrespective of the details of the environment, it is characterized by a few state variables, like temperature or chemical potential, only. This is not the case anymore, when the system is driven far away from equilibrium and the exciting question arises, whether the freedom to prepare nonthermal states of matter can be used to manipulate the properties of many-body quantum systems in a controlled fashion. Recently, this led to various interesting directions of research. In transient states, dynamically induced Bose condensation [1, 2], light-induced superconductivity [3], and dynamical phase transitions [4–6] were studied. Nonequilibrium steady states, whose properties depend on the initial condition, can occur in many-body localized isolated systems [7–11], including Floquet (time-periodically driven) systems [12, 13] such as discrete time crystals [14–18]. Floquet engineering, the coherent control of isolated systems by periodic driving on long (but finite) time scales, was very successfully used in atomic quantum gases, e.g. for the realization of artificial magnetic fields [19, 20]. Also nonequilibrium steady states of driven-dissipative many-body systems attracted considerable attention, including open Floquet systems [21–30] and photonic systems [31], where i.a. the question was studied in how far Bose condensation can be distinguished from lasing [32–34].

In this work, we investigate the nonequilibrium steady state of a quantum gas in contact with two heat baths of different temperature. In particular, we consider a one-dimensional (1D) ideal Bose gas that is coupled globally to an environment of temperature  $T$  and driven into a steady state far from equilibrium via the additional coupling to a “hot needle”, a local bath of temperature  $T_h \gg T$  [Fig. 1(a)]. We find the surprising effect that (finite-size) Bose condensation can occur when both temperatures  $T$  and  $T_h$  are orders of magnitude larger than the temperature where condensation occurs in equilibrium. We explain this behavior by a suppression of

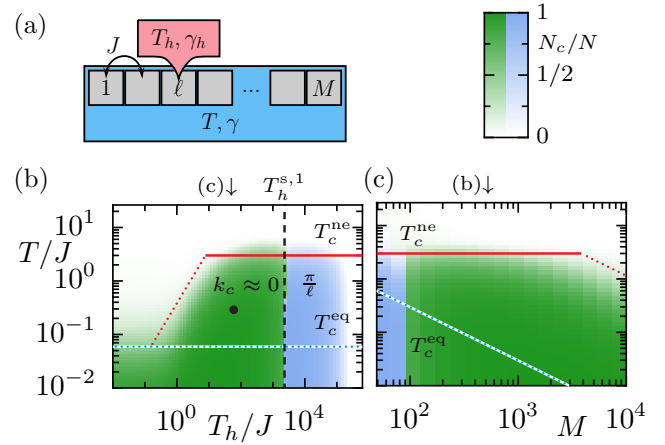


FIG. 1. (color online) (a) Tight-binding chain with  $N = nM$  bosons on  $M$  sites and tunneling parameter  $J$ , coupled with strengths  $\gamma$  and  $\gamma_h$  to a global bath of temperature  $T$  and to a “hot needle” of temperature  $T_h$  at site  $\ell$ , respectively. (b,c) Condensate fraction  $N_c/N$  indicated by green (blue) shading for ground-state (excited-state) condensation in the mode  $k_c \approx 0$  ( $k_c \approx \pi/\ell$ ) versus  $T$  and  $T_h$  or  $M$ ; for  $\ell = 5$ ,  $\gamma_h = 0.5\gamma$ ,  $n = 3$  and (b)  $M = 500$  or (c)  $T_h = 60J$ . Estimated temperature  $T_c^{ne}$  for 1D-like (3D-like) Bose condensation plotted as red dotted (solid) lines. Blue-white dotted lines give equilibrium condensation temperature  $T_c^{eq}$  (for  $\gamma_h = 0$ ). Black dashed line gives estimated needle temperature  $T_h^{s,1}$ , where excited-state condensation sets in.

long-wavelength excitations resulting from the competition between both baths. Moreover, we observe that for sufficiently large needle temperatures Bose condensation occurs in an excited state of the system, which provides a better decoupling from the hot needle. This intriguing phenomenon bears resemblance to the quantum Zeno effect.

**System and model.**—Let us consider a 1D system of  $N$  noninteracting bosons that tunnel between adjacent sites of a tight-binding chain of length  $M$  [Fig. 1(a)].

The Hamiltonian reads

$$\hat{H} = -J \sum_{i=1}^{M-1} (\hat{a}_{i+1}^\dagger \hat{a}_i + \text{h.c.}) = \sum_k \varepsilon_k \hat{n}_k. \quad (1)$$

Here  $J$  is the tunneling parameter and  $\hat{a}_i$  the bosonic annihilation operator at lattice site  $i$ . The dimensionless wave numbers  $k = \pi\nu/(M+1)$  with  $\nu = 1, \dots, M$  characterize the single-particle energy eigenmodes with energy  $\varepsilon_k = -2J \cos(k)$ , wave function  $\langle i|k \rangle = \sqrt{2/(M+1)} \sin(ki)$  (describing a superposition of states with quasimomenta  $k$  and  $-k$ ), and number operator  $\hat{n}_k = \hat{c}_k^\dagger \hat{c}_k$  with  $\hat{c}_k = \sum_i \langle k|i \rangle \hat{a}_i$ . The eigenstates of the Hamiltonian are Fock states  $|\mathbf{n}\rangle$  labeled by the vector  $\mathbf{n}$  of occupation numbers  $n_k$ .

A heat bath  $b$  is modeled as a collection of harmonic oscillators in thermal equilibrium with temperature  $T_b$  that couple to a single-particle system operator  $\hat{v}^{(b)} \equiv \sum_{qk} v_{qk}^{(b)} \hat{c}_q^\dagger \hat{c}_k$ . It is described by the Hamiltonian  $H_b = \sum_\alpha [\hbar\omega_{b\alpha} \hat{b}_{b\alpha}^\dagger \hat{b}_{b\alpha} + c_{b\alpha} (\hat{b}_{b\alpha} + \hat{b}_{b\alpha}^\dagger) \hat{v}^{(b)}]$ , with  $\omega_{b\alpha}$ ,  $c_{b\alpha}$ , and  $\hat{b}_{b\alpha}$  denoting the frequency, the coupling strength, and the lowering operator of the oscillator  $\alpha$ , respectively. In the limit of weak system-bath coupling, the bath induces quantum jumps between the energy eigenstates  $|\mathbf{n}\rangle$  of the system, where a boson is transferred from mode  $k$  to mode  $q$  with rate  $(n_q + 1)n_k R_{qk}^{(b)}$ . Here the dependence on the occupation  $n_q$  reflects the bosonic quantum statistics. The single-particle rate  $R_{qk}^{(b)}$  is obtained within the rotating-wave Born-Markov approximation and is given by the golden-rule-type expression  $R_{qk}^{(b)} = \frac{2\pi}{\hbar} |v_{qk}^{(b)}|^2 J_b(\Delta_{qk}) [\exp(\Delta_{qk}/k_B T_b) - 1]^{-1}$ , with energy difference  $\Delta_{qk} \equiv \varepsilon_q - \varepsilon_k$  and spectral density  $J_b(\Delta) = \sum_\alpha c_{b\alpha}^2 [\delta(\Delta - \hbar\omega_{b\alpha}) - \delta(\Delta + \hbar\omega_{b\alpha})]$  [35]. Setting  $\hbar = k_B = 1$  from now on, for ohmic baths with  $J_b(\Delta) \propto \Delta$  the rates take the form

$$R_{qk}^{(b)} = f_{qk}^{(b)} \gamma_b^2 \frac{\Delta_{qk}}{e^{\Delta_{qk}/T_b} - 1} \xrightarrow{T_b \gg |\Delta_{qk}|} f_{qk}^{(b)} \gamma_b^2 T_b, \quad (2)$$

with the dimensionless coupling strength  $\gamma_b$  and factor  $f_{qk}^{(b)} \propto |v_{qk}^{(b)}|^2$ . We also define the rate asymmetry

$$A_{qk}^{(b)} = R_{qk}^{(b)} - R_{kq}^{(b)} = -f_{qk}^{(b)} \gamma_b^2 \Delta_{qk}. \quad (3)$$

We will consider two baths,  $R_{qk} = R_{qk}^{(g)} + R_{qk}^{(h)}$ , a global bath  $g$  of temperature  $T$  and coupling strength  $\gamma$  as well as a hot local bath  $h$  at site  $\ell$  (the hot needle) of temperature  $T_h$  and coupling strength  $\gamma_h$  [Fig. 1(a)]. The hot needle couples to the operator  $\hat{v}^{(h)} = \hat{a}_\ell^\dagger \hat{a}_\ell$  so that  $f_{qk}^{(h)} = 4 \sin^2(\ell q) \sin^2(\ell k)$ , whereas the global bath is modeled by a collection of local baths of temperature  $T_g = T$ , each coupling to the occupation  $\hat{a}_i^\dagger \hat{a}_i$  of one site with strength  $\gamma/\sqrt{M}$ , so that  $R_{qk}^{(g)} = \sum_i R_{qk}^{(gi)}$  gives  $f_{qk}^{(g)} = \sum_i 4 \sin^2(iq) \sin^2(ik)/M \simeq 1$ .

In order to treat large systems and as a starting point of analytical approximations, we employ the meanfield approximation  $\langle \hat{n}_q \hat{n}_k \rangle \approx \langle \hat{n}_q \rangle \langle \hat{n}_k \rangle$ . It gives rise to a closed set of nonlinear kinetic equations for the mean occupations  $\langle \hat{n}_k \rangle$  from which we obtain the steady state,

$$\frac{d\langle \hat{n}_k \rangle}{dt} = \sum_q [A_{kq} \langle \hat{n}_q \rangle \langle \hat{n}_k \rangle + R_{kq} \langle \hat{n}_q \rangle - R_{qk} \langle \hat{n}_k \rangle] = 0. \quad (4)$$

In the supplemental material we compare meanfield with exact Monte-Carlo results for  $M = 50$  and find excellent agreement [36] (see also Ref. [23] for a detailed description of both methods). Note that for a fixed ratio  $\gamma_h/\gamma$ , the steady state does not depend on  $\gamma$ . After having defined the system, we are now in the position to compute the steady-state mean occupations  $\langle \hat{n}_k \rangle$  from Eq. (4).

*Finite-size equilibrium condensation.*—Let us first recapitulate the equilibrium case, where the system is coupled to a single bath of temperature  $T$  only. Here one recovers the familiar grand-canonical values  $\langle \hat{n}_k \rangle_{\text{eq}} = [e^{(\varepsilon_k - \mu)/T} - 1]^{-1}$ , where the chemical potential  $\mu$  has to be adjusted so that  $\sum_k \langle \hat{n}_k \rangle_{\text{eq}} = N$ . In the thermodynamic limit,  $M \rightarrow \infty$  at constant density  $n = N/M$ , thermal fluctuations prevent the formation of a Bose condensate in a one-dimensional system at finite temperature. However, for a finite system size  $M$ , a crossover into a Bose condensed regime with a relative occupation  $\langle \hat{n}_{k_c} \rangle/N$  of order one in the ground state  $k_c = \pi/(M+1)$  occurs when  $T$  reaches the condensation temperature  $T_c^{\text{eq}} \approx 8.3 n J/M$ , which we define as the temperature at which half of the particles occupy the single-particle ground states [36].

*High-temperature nonequilibrium condensation.*—Turning to the nonequilibrium situation with both the global bath and the hot needle present, we have to compute the steady state by solving Eq. (4) numerically. Figure 1(b) shows the condensate fraction  $N_c/N$ , with occupation  $N_c$  of the most populated mode  $k_c$ , versus both temperatures  $T$  and  $T_h$  for a system of 500 sites with  $n = 3$ ,  $\ell = 5$ , and  $\gamma_h/\gamma = 0.5$ . For small needle temperatures,  $T_h \lesssim T$ , we find a crossover into a Bose-condensed regime, roughly when the global temperature  $T$  falls below the equilibrium value  $T_c^{\text{eq}}$  (blue-white dotted line). However, when the needle temperature is *increased* further, an astonishing effect occurs: The global temperature at which condensation occurs *increases* by almost two orders of magnitude until it reaches a saturation value. Thus, for an environment well above the equilibrium condensation temperature  $T_c^{\text{eq}}$ , coupling the system to a second, even hotter local bath (the hot needle) can induce Bose condensation. When the needle temperature is increased even further, we can observe another intriguing effect. Namely, the condensate is suddenly formed in an excited state with  $k_c \approx \pi/\ell$ , as indicated by the color code. Only for very large needle temperatures, condensation eventually breaks down completely.

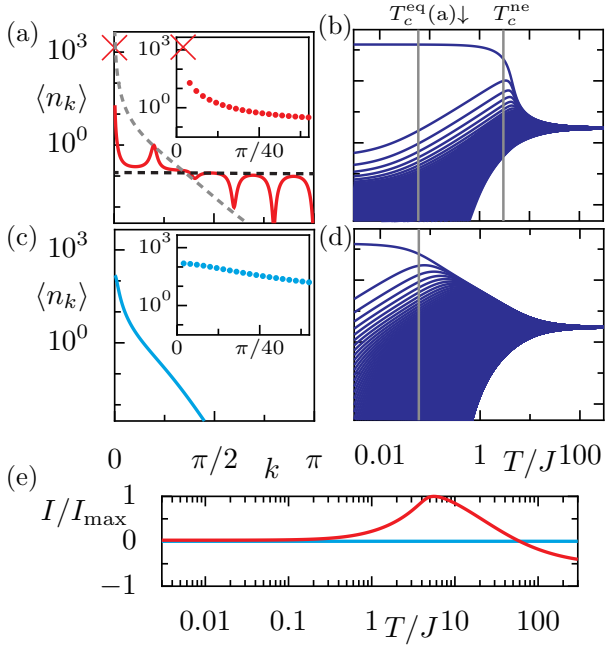


FIG. 2. (color online) (a,b) Mean occupations  $\langle n_k \rangle$  for the parameters of Fig. 1 with  $T_h = 60J$  and  $M = 500$ , (a) versus  $k$  [for  $T = 0.29J$ , black dot in Fig. 1(b)] and (b) versus  $T$ . In (a) the crosses indicate the condensate occupation, the gray (black) dashed line in the main panel shows thermal distributions for the temperature  $T$  ( $T_h$ ); the inset shows  $\langle \hat{n}_k \rangle$  for small  $k$ . (c,d) Like (a,b), but for the equilibrium situation with  $\gamma_h/\gamma = 0$ . (e) Heat current  $I$  from the needle through the system into the global bath versus  $T$  for the nonequilibrium steady state [red line, parameters like in (b)], the blue line shows the trivial equilibrium value  $I = 0$ .

In Fig. 1(c) the condensate fraction is plotted versus global temperature  $T$  and system size  $M$ . One sees that up to large system sizes of about  $10^3$  sites, condensation occurs at a large condensation temperature  $T_c^{\text{ne}}$  that is practically independent of the system size. This behavior is reminiscent of the physics of Bose condensation in a three-dimensional (3D) system. Only at even larger system sizes, the condensation temperature decreases with  $M$  resembling the equilibrium behavior in 1D. In the limit of small  $M$  ( $\lesssim 100$ ), again excited-state condensation in the mode  $k_c \approx \pi/\ell$  is found.

*Momentum distribution.*—In order to obtain a better understanding of the intriguing behavior observed in Figs. 1(b) and (c), let us have a look at the full momentum distribution  $\langle \hat{n}_k \rangle$ . It is plotted in Fig. 2(a) for the parameters indicated by the black dot in Fig. 1(b). The occupation of the condensate formed in the ground state is indicated by a red cross and the occupation of all other modes by a red line. We find an unconventional nonmonotonous behavior of  $\langle \hat{n}_k \rangle$  with equidistant peaks or dips. They are located around those wave numbers  $\kappa_\alpha = \pi\alpha/\ell$  with  $\alpha = 0, 1, \dots, \ell$  that decouple from the hot needle,  $f_{q\kappa_\alpha}^{(h)} = f_{\kappa_\alpha q}^{(h)} = 0$ . For momenta  $k \approx \kappa_\alpha$  the

distribution  $\langle \hat{n}_k \rangle$  approximately follows a thermal distribution with temperature  $T$  (dashed gray line). Between the momenta  $\kappa_\alpha$ , the distribution roughly follows the thermal distribution associated with the hot temperature  $T_h$  of the needle (dashed black line), which is rather flat. This behavior can be explained by noting that for  $|\Delta_{qk}| \ll T_b$  the rates (2) become proportional to the bath temperature, so that the occupations  $\langle \hat{n}_k \rangle$  are dominated by the hot bath with  $T_h \gg T$ , except for momenta near  $\kappa_\alpha$  that almost decouple from the needle.

This discussion gives us already an idea of the mechanism behind the high-temperature condensation induced by the needle. Namely, the width of the peak of  $\langle \hat{n}_k \rangle$  at  $k = 0$  is now determined by the competition between the global bath and the hot needle. The estimate  $w = (\gamma/\ell\gamma_h)\sqrt{T/T_h}$  for the peak width can be obtained from requiring that  $R_{qk}^{(h)} \lesssim R_{qk}^{(g)}$  for  $k < w$ . It can be small compared to the width of the thermal distribution at temperature  $T$  [Fig. 2(c)]. In this way long-wavelength excitations, which destroy Bose condensation in 1D equilibrium systems for temperatures above  $T_c^{\text{eq}}$ , are reduced. The effect of Bose condensation and the dramatic increase of the condensation temperature  $T_c$  induced by the hot needle can clearly be observed in Figs. 2(b) and (d), showing the  $T$  dependence of the occupations  $\langle \hat{n}_k \rangle$  for a system with and without coupling to the needle, respectively.

*Estimating the condensation temperature.*—Based on our qualitative discussion, we can estimate the nonequilibrium condensation temperature  $T_c^{\text{ne}}$ . In the condensate regime, where a large fraction  $N_c/N$  of the particles occupy the ground-state mode  $k_0 = \pi/(M+1)$ , the occupation of excited modes  $k \ll 1$  in the vicinity of  $k_0$  is approximately determined by  $0 \approx N_c R_{kk_0}^{(g)} + \left( A_{kk_0}^{(g)} N_c - \sum_q R_{qk}^{(h)} \right) \langle \hat{n}_k \rangle \approx N_c \gamma^2 T - 2\gamma_h^2 \ell^2 k^2 M T_h \langle \hat{n}_k \rangle$ . Here the first approximation is obtained from Eq. (4) by taking into account the coupling to the condensate mode  $k_0$  via the rates of the global bath  $R_{kk_0}^{(g)}$  (which does not decouple from  $k_0$ ) and by considering that the hot needle can transfer particles into excited modes  $q$  at distance from  $k_0$ , whose occupations can be neglected. For the second approximation we used  $\sum_q R_{qk}^{(h)} \approx 4\gamma_h^2 T_h \sin^2(\ell k) \sum_q \sin^2(\ell q) \approx 2\gamma_h^2 \ell^2 k^2 M T_h \gg A_{kk_0}^{(g)} N_c$  and the small- $|\Delta_{kq}|/T$  expression (2) for the rates  $R_{kk_0}^{(g)}$ . With that, the condensate depletion  $N' = \sum_{k \neq k_0} \langle \hat{n}_k \rangle$  is approximately given by  $N' \approx N_c w^2 \frac{M}{2\pi^2} \sum_{\nu=2}^{\infty} \frac{1}{\nu^2}$  and the condensation temperature, defined by  $N' = N_c$ , can be estimated to read  $T_c^{\text{ne1}} \approx 30.6 \frac{\ell^2 \gamma_h^2 T_h}{\gamma^2} \frac{1}{M}$ . It is plotted as red dotted line in Figs. 1(b) and (c) and agrees well with the observed behavior. Like in equilibrium in 1D, also the nonequilibrium condensation relies on the infrared cutoff given by the inverse system size.

However, in contrast to equilibrium, in the nonequi-

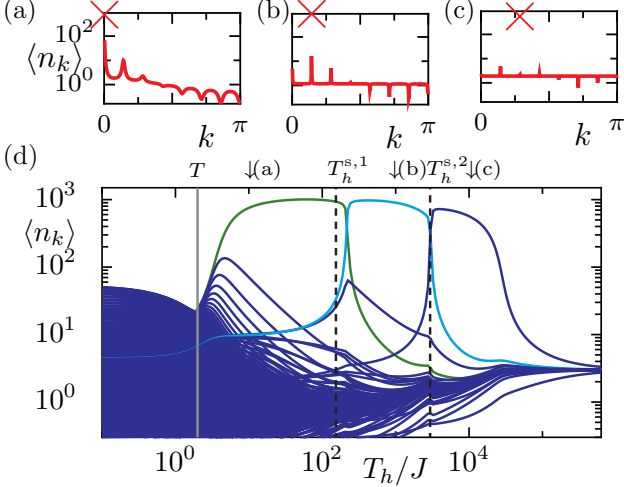


FIG. 3. (color online) Mode occupations (d) versus needle temperature  $T_h$  for  $T = 2J$ ,  $\ell = 7$ ,  $M = 500$ ,  $n = 3$ , and  $\gamma_h/\gamma = 1$ . With increasing  $T_h$  the system passes from a state without Bose condensate through a sequence of states with a condensate in the states  $k_0 \approx 0$  (green line),  $k_1 \approx \pi/\ell$  (light blue line), and  $k_2 \approx 2\pi/\ell$  (violet line), before condensation breaks eventually down again. (a-c) Momentum distribution for states with condensates in three different modes.

librium steady state Bose condensation can also be destroyed by increasing the occupation of modes with large momenta  $q$ , which couple to the condensate via the rates induced by the global bath. This effect can be estimated by considering the regime  $T \ll T_c^{\text{ne}1}$ , where the total occupation of excited long-wavelength modes is suppressed by the finite system size  $M$ , so that we can approximate the occupation of excited states by the flat distribution  $\langle \hat{n}_q \rangle \approx N'/M$  induced by the dominant hot-needle bath [dashed black line in Fig. 2(a)]. With these assumptions, we obtain  $0 \approx \sum_{q \neq k_0} [N_c(A_{k_0q}^{(g)} N'/M - R_{qk_0}^{(g)}) + R_{k_0q}^{(g)} N'/M] \approx \gamma^2 N_c(2JN' - TM)$ , where for the second approximation, we employed Eq. (3) and the asymptotic expression in Eq. (2), neglected the last term, and used  $\sum_q \Delta_{qk_0} \approx 2JM$ . Solving this equation for  $N_c = N' = nM/2$ , one finds the condensation temperature  $T_c^{\text{ne}2} \approx nJ$ , which is plotted as red solid line in Fig. 1(b) and (c). The fact that it does not depend on the system size, reflects similarity to the break-down of Bose condensation in a 3D system in equilibrium, which is not driven by long-wavelength modes either.

*Excited-state condensation.*—Figure 3(d) shows how the occupations depend on the needle temperature  $T_h$  for a system with  $\gamma_h/\gamma = 1$ ,  $M = 500$ ,  $\ell = 7$ , and  $T = 2J$ . Since the global temperature  $T$  lies well above the equilibrium condensation temperature  $T_c^{\text{eq}} \approx 0.05J$ , no Bose condensate is found at  $T_h = T$ , where the system is in equilibrium. However, when  $T_h$  is increased, soon ground-state Bose condensation sets in. When the needle temperature is increased further, remarkably a Bose

condensate in the excited mode  $k \approx \pi/\ell$  supersedes the ground-state condensate at a switch temperature  $T_h^{s,1}$ . The condensate mode switches once more to  $k \approx 2\pi/\ell$  at  $T_h^{s,2}$ , before eventually at very large needle temperatures  $T_h \gtrsim 10^4 J$  condensation breaks down again. The panels (a), (b), and (c) depict the momentum distribution for the three different needle temperatures marked in (d) and clearly show condensation in three different modes.

We find that the switching of the condensate mode is triggered by the possibility to reduce the coupling between the condensate mode and the hot needle. Namely, typically the allowed wave numbers  $k = \nu\pi/(M+1)$  that comply with the boundary conditions, do not assume those values  $\kappa_\alpha$  that would perfectly decouple from the hot needle. We denote by  $k_\alpha$  the allowed wavenumber that minimizes the distance  $\delta_\alpha = |k - \kappa_\alpha|$ , which quantifies the coupling,  $f_{qk_\alpha}^{(h)} \simeq 4\sin^2(\ell q)\ell^2\delta_\alpha^2$ . With increasing  $T_h$  we generally find a sequence of condensate modes  $k_0, k_{\alpha_1}, k_{\alpha_2}, \dots$ , where  $\alpha_{j+1}$  is the smallest value of  $\alpha$  with  $\alpha > \alpha_j$  and  $\delta_\alpha < \delta_{\alpha_j}$ . The sequence ends, when the coupling cannot be lowered anymore by a larger  $k_\alpha$ . Since one has  $\delta_0 = k_0$  for the ground state  $k_0$  and fluctuating values  $\delta_\alpha \leq \delta_0/2$  (depending on  $M$  and  $\ell$ ) for  $\alpha \geq 1$ , one always finds at least one switch of the condensate mode and  $\alpha_1 = 1$ . While for the parameters of Fig. 1(b) the sequence ends already with  $k_1$ , it ends with  $k_2$  for the parameters of Fig. 3 (for  $\ell = 21$  and  $M = 200$ , we e.g. observe the sequence  $\alpha = 0, 1, 2, 7$ , not shown).

We can estimate the switch temperature  $T_h^{s,\alpha}$ , above which a condensate in mode  $k_\alpha$  forms. Assuming a condensate with  $\langle \hat{n}_{k_\alpha} \rangle \approx N$  particles in mode  $k_\alpha$ , the momentum distribution can formally be written like  $\langle \hat{n}_k \rangle = \sum_q R_{kq} \langle \hat{n}_q \rangle / B_k$  with  $B_k = \sum_q [A_{qk} \langle \hat{n}_q \rangle + R_{qk}] \approx A_{k_\alpha k} N + \sum_q R_{qk}^{(h)} \approx \gamma^2 \Delta_{kk_\alpha} N + 2M\gamma_h^2 \sin^2(\ell k) T_h$ , where we employed similar approximations as before. Physical occupations  $\langle \hat{n}_k \rangle \geq 0$  require  $B_k > 0$ . The first term contributing to  $B_k$  becomes negative for  $k < k_\alpha$  and has to be compensated by the second term, which is positive but small for  $k = k_{\alpha'}$  where  $\sin^2(\ell k_{\alpha'}) \simeq \ell^2 \delta_{\alpha'}^2 \sim \ell^2/M^2$ . The temperature  $T_h$  above which  $\langle \hat{n}_{k_{\alpha'}} \rangle \geq 0$  for all  $\alpha' < \alpha$  provides a good estimate for the switch temperature,  $T_h^{s,\alpha} \approx 0.5n(\gamma/\ell\gamma_h)^2 \max_{\alpha' < \alpha} (\Delta_{k_\alpha k_{\alpha'}}/\delta_{\alpha'}^2)$ , see dashed lines in Fig. 3(d) and Fig. 1(b). The linear dependence of  $T_h^{s,\alpha}$  on  $n$  indicates that excited-state condensation is suppressed (shifted to  $T_h = \infty$ ) in the limit of high densities, where ground-state condensation is expected for a system coupled to two thermal baths (of positive temperature) [22, 23].

*General picture and conclusion.*—An intuitive interpretation of the high-temperature and excited-state Bose condensation observed here is that the nonequilibrium condensation can also be viewed as a mechanism that suppresses the heat influx  $I_h$  from the hot bath, with  $I_b = \sum_{qk} \Delta_{qk} R_{qk}^{(b)} (\langle \hat{n}_q \rangle + 1) \langle \hat{n}_k \rangle$ . Namely, keeping the distribution  $\langle \hat{n}_k \rangle$  fixed,  $I_h$  would increase linearly with

$T_h$  [according to Eq. (2)], while it still has to be balanced by the outflux  $I_g$  into the colder global bath (since  $I_h = -I_g$  for a steady state). This increase is prevented by forming of a condensate in a mode that almost decouples from the hot needle. This interpretation is supported by Fig. 2(e) showing that the heat current  $I = I_h = -I_g$  through the system plotted versus  $T$  shows a maximum near the condensation temperature and, thus, a negative differential heat conductivity in the condensed regime. This counterintuitive effect is explained by noting that the number of particles contributing to the heat transport is reduced by condensing into the ground state  $k_0$ , which hardly couples to the hot needle. The onset first of ground-state condensation and later also of excited-state condensation observed when the needle temperature  $T_h$  is increased [Fig. 3(d)] can, therefore, be understood as a strategy of the system to minimize its coupling to the hot needle (and with that  $I_h$ ) further and further. Note that these intriguing effects do not rely on the discrete nature of the tight-binding chain considered here and, therefore, occur equally in a continuous system [36].

The tendency to avoid a state with strong coupling to the environment bears resemblance to the quantum Zeno effect [37]. The underlying mechanism, that the coupling to a second very hot bath can lead to a depletion of some system modes and, thus, to an enhanced occupation (and quantum degeneracy) of the subsystem defined by all other modes (not necessarily including the ground state), should be rather universal. It suggests a general strategy for the robust preparation of quantum degenerate nonequilibrium states with unconventional properties and also in large-temperature environments. In future work, it will be interesting to explore such possibilities in bosonic and fermionic quantum systems. This includes the investigation of interacting systems and the role of strong system-bath coupling.

*Acknowledgment.*—We acknowledge discussion with Toni Ehmcke. This work was supported by the German Research Foundation DFG (FOR 2414). D. V. is grateful for support by the Studienstiftung des deutschen Volkes.

---

\* Electronic address: schnell@pks.mpg.de

† Electronic address: eckardt@pks.mpg.de

- [1] M. Rigol and A. Muramatsu, Phys. Rev. Lett. **93**, 230404 (2004).
- [2] L. Vidmar, J. P. Ronzheimer, M. Schreiber, S. Braun, S. S. Hodgman, S. Langer, F. Heidrich-Meisner, I. Bloch, and U. Schneider, Phys. Rev. Lett. **115**, 175301 (2015).
- [3] M. Mitrano, A. Cantaluppi, D. Nicoletti, S. Kaiser, A. Perucchi, S. Lupi, P. D. Pietro, D. Pontiroli, M. Ricco, S. R. Clark, D. Jaksch, and A. Cavalleri, Nature **530**, 461 (2016).
- [4] M. Heyl, A. Polkovnikov, and S. Kehrein, Phys. Rev. Lett. **110**, 135704 (2013).
- [5] P. Jurcevic, H. Shen, P. Hauke, C. Maier, T. Brydges,

- C. Hempel, B. P. Lanyon, M. Heyl, R. Blatt, and C. F. Roos, arXiv:1612.06902 (2016).
- [6] N. Fläschner, D. Vogel, M. Tarnowski, B. S. Rem, D.-S. Lümman, M. Heyl, J. C. Budich, L. Mathey, K. Sengstock, and C. Weitenberg, arXiv:1608.05616 (2016).
- [7] D. M. Basko, I. L. Aleiner, and B. L. Altshuler, Ann. Phys. **321**, 1126 (2006).
- [8] R. Nandkishore and D. A. Huse, Ann. Rev. Cond. Mat. Phys. **6**, 15 (2015).
- [9] M. Schreiber, S. S. Hodgman, P. Bordia, H. P. Lschen, M. H. Fischer, R. Vosk, E. Altman, U. Schneider, and I. Bloch, Science **349**, 842 (2015).
- [10] J. Smith, A. Lee, P. Richerme, B. Neyenhuis, P. W. Hess, P. Hauke, M. Heyl, D. A. Huse, and C. Monroe, Nat. Phys. **12**, 907 (2016).
- [11] J.-y. Choi, S. Hild, J. Zeiher, P. Schauš, A. Rubio-Abadal, T. Yefsah, V. Khemani, D. A. Huse, I. Bloch, and C. Gross, Science **352**, 1547 (2016).
- [12] P. Ponte, Z. Papić, F. m. c. Huveneers, and D. A. Abanin, Phys. Rev. Lett. **114**, 140401 (2015).
- [13] A. Lazarides, A. Das, and R. Moessner, Phys. Rev. Lett. **115**, 030402 (2015).
- [14] V. Khemani, A. Lazarides, R. Moessner, and S. L. Sondhi, Phys. Rev. Lett. **116**, 250401 (2016).
- [15] C. W. von Keyserlingk, V. Khemani, and S. L. Sondhi, Phys. Rev. B **94**, 085112 (2016).
- [16] D. V. Else, B. Bauer, and C. Nayak, Phys. Rev. Lett. **117**, 090402 (2016).
- [17] J. Zhang, P. W. Hess, A. Kyprianidis, P. Becker, A. Lee, J. Smith, G. Pagano, I.-D. Potirniche, A. C. Potter, A. Vishwanath, N. Y. Yao, and C. Monroe, Nature **543**, 217 (2017).
- [18] S. Choi, J. Choi, R. Landig, G. Kucsko, H. Zhou, J. Isoya, F. Jelezko, S. Onoda, H. Sumiya, V. Khemani, C. von Keyserlingk, N. Y. Yao, E. Demler, and M. D. Lukin, Nature **543**, 221 (2017).
- [19] M. Bukov, L. D'Alessio, and A. Polkovnikov, Adv. in Phys. **64**, 139 (2015).
- [20] A. Eckardt, Rev. Mod. Phys. **89**, 011004 (2017).
- [21] N. Tsuji, T. Oka, and H. Aoki, Phys. Rev. Lett. **103**, 047403 (2009).
- [22] D. Vorberg, W. Wustmann, R. Ketzmerick, and A. Eckardt, Phys. Rev. Lett. **111**, 240405 (2013).
- [23] D. Vorberg, W. Wustmann, H. Schomerus, R. Ketzmerick, and A. Eckardt, Phys. Rev. E **92**, 062119 (2015).
- [24] L. E. F. Foa Torres, P. M. Perez-Piskunow, C. A. Balseiro, and G. Usaj, Phys. Rev. Lett. **113**, 266801 (2014).
- [25] K. I. Seetharam, C.-E. Bardyn, N. H. Lindner, M. S. Rudner, and G. Refael, Phys. Rev. X **5**, 041050 (2015).
- [26] H. Dehghani, T. Oka, and A. Mitra, Phys. Rev. B **91**, 155422 (2015).
- [27] G. Goldstein, C. Aron, and C. Chamon, Phys. Rev. B **92**, 174418 (2015).
- [28] T. Iadecola, T. Neupert, and C. Chamon, Phys. Rev. B **91**, 235133 (2015).
- [29] T. Shirai, J. Thingna, T. Mori, S. Denisov, P. Hänggi, and S. Miyashita, New J. Phys. **18**, 053008 (2016).
- [30] T. Qin and W. Hofstetter, arXiv:1704.03250 (2017).
- [31] I. Carusotto and C. Ciuti, Rev. Mod. Phys. **85**, 299 (2013).
- [32] J. Klaers, J. Schmitt, F. Vewinger, and M. Weitz, Nature **468**, 545 (2010).
- [33] T. Byrnes, N. Y. Kim, and Y. Yamamoto, Nature Phys. **10**, 803 (2014).

- [34] H. A. M. Leymann, D. Vorberg, T. Lettau, C. Hopfmann, C. Schneider, M. Kamp, S. Höfling, R. Ketzmerick, J. Wiersig, S. Reitzenstein, and A. Eckardt, arXiv:1612.04312 (2017).
- [35] H. Breuer and F. Petruccione, *The Theory of Open Quantum Systems* (Oxford University Press, Oxford & New York, 2002).
- [36] Additional information regarding equilibrium condensation, a comparison to exact Monte-Carlo simulations, and the physics of a continuous 1D system can be found in the supplemental material.
- [37] B. Misra and E. C. G. Sudarshan, J. Math. Phys. **18**, 756 (1977).

# Supplemental material for “High-temperature nonequilibrium Bose condensation induced by a hot needle”

Alexander Schnell,<sup>1,\*</sup> Daniel Vorberg,<sup>1</sup> Roland Ketzmerick,<sup>1,2</sup> and André Eckardt<sup>1,†</sup>

<sup>1</sup>*Max-Planck-Institut für Physik komplexer Systeme, Nöthnitzer Straße 38, 01187 Dresden, Germany*

<sup>2</sup>*Technische Universität Dresden, Institut für Theoretische Physik and Center for Dynamics, 01062 Dresden, Germany*

(Dated: May 17, 2022)

In this supplemental material we (i) estimate the condensation temperature for a one-dimensional tight-binding chain of finite length  $M$  in equilibrium; (ii) justify the kinetic equations of motion obtained from the meanfield approximation by comparing it to Monte-Carlo results for the exact master equation; and (iii) show that the nonequilibrium condensation phenomena found for a discrete tight-binding chain can also be observed in a continuous one-dimensional system.

## CONDENSATION TEMPERATURE IN EQUILIBRIUM

Under equilibrium conditions, when the system is coupled only to the global bath of temperature  $T$  (i.e. for  $\gamma_h = 0$ ), Equation (4) (of the main text) is solved by the grand-canonical mean occupations

$$\langle \hat{n}_k \rangle = \frac{1}{e^{(\varepsilon_k - \mu)/T} - 1} \quad (\text{A.1})$$

with chemical potential  $\mu$ . When (finite-size) Bose condensation sets in,  $\mu$  approaches  $\varepsilon_{k_0}$  from below, so that the occupations of the low-energy modes with  $k \ll 1$  can be approximated by

$$\langle \hat{n}_k \rangle \simeq \frac{T}{\varepsilon_k - \mu} \simeq \frac{T}{Jk^2 - 2J - \mu}, \quad (\text{A.2})$$

where we have used  $\varepsilon_k = -2J \cos(k) \simeq -2J + Jk^2$ . The chemical potential can be expressed in terms of the occupation  $N_c = \langle \hat{n}_{k_0} \rangle$  of the ground state with wave number  $k_0 = \pi/(M+1)$ ,

$$\mu = -2J + Jk_0^2 - T/N_c. \quad (\text{A.3})$$

For low temperatures, the number  $N'$  of particles occupying excited states, with  $k = \nu\pi/(M+1)$ , is dominated by the long-wavelength modes, so that we can approximate

$$N' = \sum_{k' \neq k_0} \langle \hat{n}_k \rangle \simeq \sum_{\nu=2}^{\infty} \frac{1}{\frac{J\pi^2}{TM^2}(\nu^2 - 1) + \frac{1}{N_c}}. \quad (\text{A.4})$$

For a finite system, we define the characteristic temperature  $T_c$ , where Bose condensation sets in, as the temperature for which half of the particles occupy the single-particle ground state,  $N' = N_c = N/2$ . It is given by

$$T_c^{\text{eq}} \simeq \frac{a\pi^2}{2} \frac{nJ}{M} \approx 8.3 \frac{nJ}{M}, \quad (\text{A.5})$$

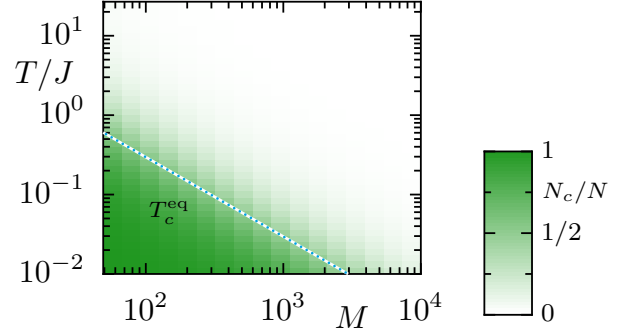


FIG. 1. Condensate fraction  $N_c/N$  for a tight binding chain of  $M$  sites at temperature  $T$  (shading). The blue-white dotted line gives the analytical estimate for the condensation temperature, where half of the particles occupy the single-particle ground state.

where  $a \approx 1.68$  solves  $1 = a \sum_{\nu=2}^{\infty} 1/(\nu^2 + a - 1)$ . In Fig. 1 we plot the ground-state occupation (i.e. the condensate fraction) of the tight binding chain together with the estimate (A.5) for the condensation temperature  $T_c^{\text{eq}}$ . The inverse dependence of  $T_c^{\text{eq}}$  on the system size  $M$  reflects the well-known result that in one spatial dimension, in the thermodynamic limit Bose-Einstein condensation is suppressed by thermal long-wavelength fluctuations.

## QUASIEXACT MONTE-CARLO RESULTS FOR A SMALL SYSTEM

The meanfield approximation  $\langle \hat{n}_q \hat{n}_k \rangle \approx \langle \hat{n}_q \rangle \langle \hat{n}_k \rangle$ , which gives rise to the closed set of kinetic equations (4) for the mean occupations, allows us to treat large systems of up to  $M = 10^4$  lattice sites and to find analytical estimates for the parameters where condensation sets in. In order to justify this approximation, we have also simulated the full many-body rate equation for the probability distribution  $p_{\mathbf{n}}$  for finding the system in the eigenstate  $|\mathbf{n}\rangle$ . It reads

$$\dot{p}_{\mathbf{n}} = \sum_{kq} (1 + n_q) n_k (R_{kq} p_{\mathbf{n}_{q \leftarrow k}} - R_{qk} p_{\mathbf{n}}), \quad (\text{A.6})$$

where  $\mathbf{n}_{q \leftarrow k}$  denotes the vector of occupation numbers obtained from  $\mathbf{n}$  by transferring a particle from mode  $k$  to mode  $q$ .

An efficient way of solving this equation is given by quantum-jump Monte-Carlo simulations (see, e.g., [1]). For that purpose we generate a random walk in the classical space of Fock states  $\mathbf{n}$  (which is exponentially large with respect to the system size, but much smaller than the Fock space, which contains also the coherent superpositions of the Fock states). Namely, according to the sum and the relative weight of the many-body rates  $R_{qk}(n_q + 1)n_k$  leading away from the current state  $\mathbf{n}$ , we draw both the time after which a quantum jump happens and the new state  $\mathbf{n}_{q \leftarrow k}$ , respectively. Expectation values like the mean occupations  $\langle \hat{n}_k \rangle$  are computed by averaging over a random path. This method gives quasiexact results, in the sense that the accuracy is controlled by the length of the random path. A detailed description of the method is given in Ref. [2].

In Fig. 2 we plot the mean occupations  $\langle \hat{n}_k \rangle$  of a system of  $M = 50$  sites and  $n = 3$ ,  $\ell = 3$ ,  $\gamma_h/\gamma = 1$ , and  $T_h = 120J$ . The Monte-Carlo data (red crosses) are reproduced almost perfectly by the meanfield solution (solid lines). Already in this rather small system, we can see a rather sharp crossover, to a Bose condensed regime at  $T_c^{\text{ne}}$ .

### CONTINUOUS SYSTEM

In the main text, we treated a one-dimensional (1D) system of noninteracting bosons in a tight-binding lattice. However, the effects discussed in the main text do not depend on the discrete nature of the tight-binding

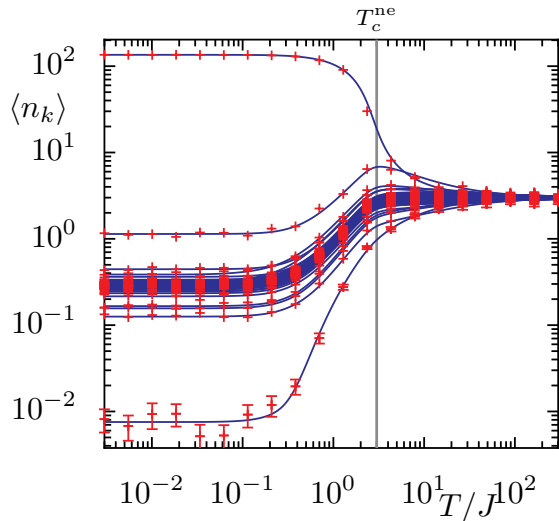


FIG. 2. Mean occupations  $\langle n_k \rangle$  for a system with  $M = 50$ ,  $n = 3$ ,  $\ell = 3$ ,  $\gamma = \gamma_h$ ,  $T_h = 120J$ . Crosses represent the Monte-Carlo results. We show error bars for the least occupied state only, because for the other states they are too small to be visible. The data is well approximated by the solid lines which result from the meanfield approximation.

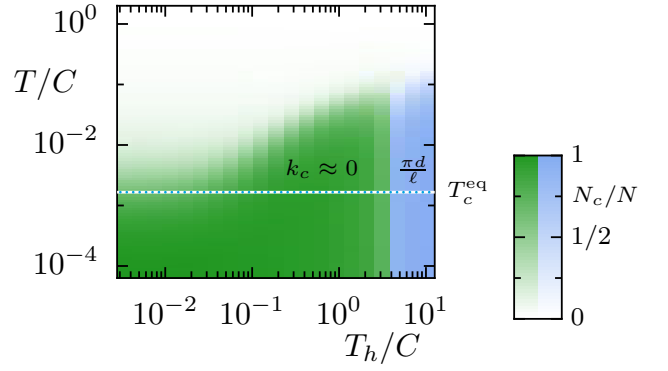


FIG. 3. Condensate fraction  $N_c/N$  for the continuous 1D system of length  $L = 500d$  and density of  $n = 0.1/d$  versus the temperatures  $T$  and  $T_h$  of the global bath and the hot needle, respectively. The spatial extent of the hot needle is  $d$  and it is placed at distance  $\ell = 20d$  from the edge. The relative coupling between both baths is  $\gamma_h/\gamma = 1/4$ . Green (light blue) shading indicates the relative number of particles in the mode  $k_0 \approx 0$  ( $k_1 \approx \pi d/\ell$ ). The blue-white dotted line corresponds to the condensation temperature in equilibrium.

lattice. They occur in a similar form also in a continuous system one-dimensional system described by the Hamiltonian

$$\hat{H} = \int_0^L dx \hat{\psi}^\dagger(x) \left( -\frac{\hbar^2}{2m} \frac{d^2}{dx^2} \right) \hat{\psi}(x) = \sum_k \varepsilon_k \hat{n}_k, \quad (\text{A.7})$$

where  $m$  denotes the mass of the particles and  $\hat{\psi}(x)$  the field operator annihilating a boson at position  $x$ . The dimensionless wavenumbers  $k = \nu\pi d/L$  with  $\nu = 1, 2, \dots$  and some length scale  $d$  (which we take to be the extent of the hot needle defined below) characterize the single-particle eigenstates with energy  $\varepsilon_k = \frac{\hbar^2 k^2}{2md^2} \equiv Ck^2$ , and wave functions  $\langle x|k \rangle = \sqrt{2/L} \sin(kx/d)$ . The corresponding number operator reads  $\hat{n}_k = \hat{c}_k^\dagger \hat{c}_k$  with  $\hat{c}_k = \int_0^L dx \langle k|x \rangle \hat{\psi}(x)$ . The energy eigenstates of the system are Fock states  $|\mathbf{n}\rangle$  labeled by the vector of occupation numbers  $n_k$ .

In such a continuous system, a hot local bath at position  $x = \ell$  of spatial extent  $d$ , can be described by the coupling operator

$$\hat{v}_h = \frac{L}{d} \int_{\ell-d/2}^{\ell+d/2} dx \hat{\psi}^\dagger(x) \hat{\psi}(x). \quad (\text{A.8})$$

The corresponding single-particle rates are of the form of Eq. (2), with  $f_{kq}^{(h)} = [\cos(k\frac{\ell}{d}) \text{sinc}(k/2) - \cos(q\frac{\ell}{d}) \text{sinc}(q/2)]^2$  giving  $f_{kq}^{(h)} \simeq 4 \sin^2(k\ell/d) \sin^2(q\ell/d)$  in the limit  $d \rightarrow 0$ . A global heat bath is still described by Eq. (2) with  $f_{kq}^{(g)} = 1$ .

From these rates we computed the corresponding mean-occupations for a system of  $N = 0.1L/d$  particles, length  $L = 500d$ , and needle position  $\ell = 20d$ . In

Fig. 3 we plot the condensate fraction, i.e. the fraction of particles occupying the most occupied mode whose wave number is indicated by the color of the shading (green for  $k_0 \approx 0$  and light blue for  $k_1 \approx \pi d/\ell$ ). As for the tight-binding chain, we can clearly see that the temperature of the global bath at which the system condenses increases with needle temperature. As a result Bose condensation is found for a system coupled to two baths both having temperatures well above the equilibrium condensation temperature  $T_c^{\text{ne}}$  (which is indicated as blue-white dotted line). Moreover, when the needle temperature is increased further, ground-state condensation in mode

$k_0 \approx 0$  is superseded by the formation of a condensate in the excited mode  $k_1 \approx \pi d/\ell$ , which provides a better decoupling from the hot needle.

---

\* Electronic address: schnell@pks.mpg.de

† Electronic address: eckardt@pks.mpg.de

- [1] M. B. Plenio and P. L. Knight, Rev. Mod. Phys. **70**, 101 (1998).
- [2] D. Vorberg, W. Wustmann, H. Schomerus, R. Ketzmerick, and A. Eckardt, Phys. Rev. E **92**, 062119 (2015).